Dynamic Head-Disk Interface Instabilities With Friction for Light Contact (Surfing) Recording

Vakis, Antonis I.; Lee, Sung-Chang; Polycarpou, Andreas A.

Published in:
IEEE Transactions on Magnetics

DOI:
10.1109/TMAG.2009.2029410

Publication date:
2009

Dynamic Head-Disk Interface Instabilities With Friction for Light Contact (Surfing) Recording

Antonis I. Vakis[1], Sung-Chang Lee[2], and Andreas A. Polycarpou[1]

[1]Department of Mechanical Science and Engineering, University of Illinois at Urbana-Champaign, Urbana, IL 61801 USA
[2]Samsung Information Systems America, San Jose, CA 95134 USA

Recent advances in hard-disk drive technology involve the use of a thermal fly-height control (TFC) pole tip protrusion to bring the read/write recording elements of the slider closer to the disk surface and thus achieve Terabit per square inch recording densities. A dynamic, contact mechanics-based friction model of the head-disk interface (HDI) that includes roughness and accounts for the TFC geometry and its influence on the HDI dynamics is presented. The model is based on physical parameters and does not include any empirical coefficients. Experimental flyability/touchdown measurements were performed and used to examine in detail the HDI contact criterion in the presence of surface roughness and dynamic microwaviness. Using the model, a procedure is outlined that identifies the optimal clearance and light contact conditions, i.e., the amount of thermal actuation that minimizes, both, the clearance, as well as the flying height modulation. Through calculation of the time varying interfacial forces, mean pressure and shear stress at the HDI can be predicted and used to characterize the contact regime. Based on our results, a light contact regime with reduced bouncing vibrations and low stresses (thus, low wear) that would enable surfing recording is identified.

Index Terms—**Dynamic model, friction, hard-disk drive (HDD), head-disk interface (HDI), thermal fly-height control (TFC).**

I. Introduction

THERMAL fly-height control (TFC) describes technology that enables ultra-high density recordings in hard-disk drives (HDD) by thermomechanically actuating the read/write elements of the slider closer to the rotating disk surface [1]. Using TFC technology, the slider body flies at a predescribed nominal flying height of the order of 10 nm away from the rotating disk surface, reducing the clearance between the read/write element and the disk surface to less than few nm, thus, enabling higher recording densities. A dynamic contact model was developed to account for the exact TFC geometry that affects the calculation of the nominal area of contact as well as the dynamically changing separation and interfacial forces. Measured dynamic microwaviness (DMW), roughness and material parameters are used as inputs to the dynamic contact/ friction model.

The improved subboundary lubrication (ISBL) contact model was implemented in the dynamic simulations [2]. The model uses physics-based formulations for adhesion, contact and friction forces with respect to the separation between an equivalent smooth flat and a rough surface. The forces are dimensionalized with respect to the nominal area of contact, which is analytically calculated for a specific TFC geometry as a function of protrusion height. Chen and Bogy [3] and Yu *et al.* [4] have presented similar models investigating TFC flyability and partial contact with similar predictions. In the present work the surface roughness and material properties are the only inputs to the calculation of the interfacial forces, without the use of empirical coefficients. Using the improved dynamic contact model with the exact TFC geometry, we investigated the identification and definition of the contact criterion as a function of surface roughness. The onset of contact was correlated with touchdown (TD) experiments using TFC sliders. Using a lumped parameter 2-DOF nonlinear dynamic head-disk interface (HDI) model, we obtain the instantaneous normal separation h, which is used in the ISBL model to calculate the time varying interfacial forces; these, in turn, are used to obtain the instantaneous mean contact pressure and shear stress, which determine stable flyability and long term wear.

Manuscript received February 05, 2009. Current version published October 23, 2009. Corresponding author: A. A. Polycarpou (e-mail: polycarpou@illinois.edu).

Digital Object Identifier 10.1109/TMAG.2009.2029410

II. 2-DOF Dynamic Contact Model With Friction

A. Dynamic HDI Model With TFC

In an earlier dynamic HDI model without TFC [2], when the slider is flying without contacting the disk, a nonlinear air bearing force F_{ar} is acting together with a linear damping force on the trailing edge. An analogous air bearing force is acting on the leading edge of the slider with both the stiffness and damping terms being linear. Under flying equilibrium conditions, the slider dynamics are dependent upon the air-bearing and adhesive forces as well as the suspension dynamics. When contact occurs, a contact force F_c, calculated from the roughness parameters and modeled as nonlinear contact stiffness k_c and linear damping c_c, together with a friction force Q, are added to the force balance at the point of contact.

The model presented in [2] was modified such that the lowest point of the TFC protrusion becomes the point of contact. The TFC protrusion is modeled as an ellipsoid that has a fixed base profile with its height relative to the bottom of the slider being the only changing variable. The exact shape of the TFC geometry (bulge) could be accurately predicted using, for example, finite element analysis. Using such data, one can then extract the geometry of the top surface of the bulge that is engaged during contact and use it to construct the ellipsoidal TFC model, as done in the present work. The TFC geometry model is characterized by four parameters: $\mathrm{a_{TFC}}$, b_{TFC}, w_{TFC} and x_{TFC}. For the specific TFC design used in this work, the half-width $\mathrm{a_{TFC}}$

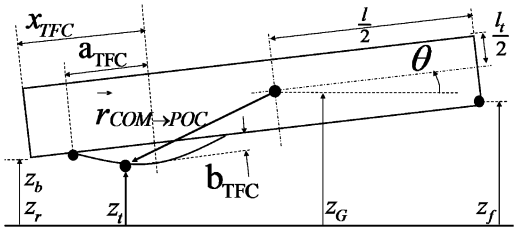

Fig. 1. Schematic of slider showing the TFC pole tip protrusion (exaggerated size) with relevant dimensions and displacements from the roughness mean plane.

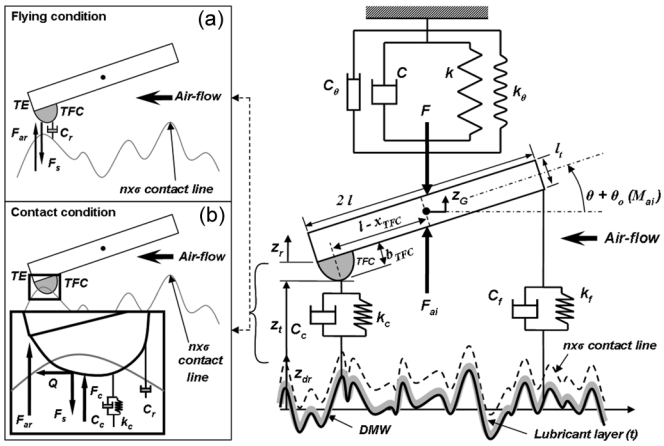

Fig. 2. Free body diagram of the 2-DOF dynamic contacting system. (a) Flying condition. (b) Contacting condition.

was measured to be equal to 3 μm; the distance of the TFC ellipsoid from the trailing edge x_{TFC} was equal to 8 μm; and, the width in the direction perpendicular to the plane (shown in Fig. 1) w_{TFC} is equal to 50 μm. The TFC bulge height b_{TFC} varies between zero (no actuation) and 15 nm (maximum actuation). The TFC protrusion height is of the order of few nm as opposed to the TFC base dimensions that are of the order of few μm; hence, the TFC protrusion height is greatly exaggerated in Fig. 1. The contact and friction forces are acting on the lowest instantaneous point of the TFC protrusion, whose position can be accurately described in terms of a fixed reference point such as the trailing edge.

Fig. 2 depicts the 2-DOF dynamic model of the HDI with the TFC protrusion along with the interfacial forces developed during different characteristic states. The first state, labeled as *flying condition*, is characterized by the slider flying over the disk without contact under the influence of the air-bearing and adhesive forces. The adhesive force is acting on the TFC situated close to the trailing edge as shown in inset a) of Fig. 2. The second state, labeled as *contact condition*, occurs when the TFC contacts the disk based on the established contact criterion. In this case, in addition to the air-bearing and adhesive forces, contact and friction forces are also acting on the TFC as shown in inset b) of Fig. 2.

B. ISBL Interfacial (Contact- Adhesion-Friction) Models

The interfacial model including roughness was presented elsewhere, e.g., [2], and is used to calculate the adhesion, contact and friction forces as well as the real area of contact using roughness, material and lubricant properties. The model does not assume a predefined friction coefficient value but instead calculates it directly from the interfacial forces. The total adhesive force is calculated from the individual asperity contributions using a statistical Greenwood-Williamson-type (includes plastic deformation) roughness model. The total adhesive force combines the contributions from non-contacting asperities, lubricant contacting asperities (lubricant layer is strongly adhered to the surface), and elastically and elastically-plastically deforming asperities.

The total normal contact force calculation considers the contribution of elastic, elastic-plastic and fully-plastic contacts. The model assumes that the lubricant layer is displaced during contact and the contact force is not affected by the presence of the thin lubricant layer, i.e., the contact force is due to the asperity deformation. Further improvements in the model should also include the lubricant contact/friction forces. The total friction force is calculated based on the contributions of elastically and elastically plastically deforming asperities. The real area of contact is calculated from the contributions of elastically, elastically plastically, and fully plastically contacting asperities.

C. Air Bearing Stiffness and Model Parameters

The complex nature of a slider air bearing is best described by three degrees-of-freedom, i.e. vertical, pitch and roll motions, through a generalized Reynolds pressure field equation beneath the air-bearing surface. A 2-DOF model including the vertical and pitch modes is adequate for capturing the basic dynamic air-bearing behavior [2], which is adopted in this work. In the present model, it is assumed that the slider maintains the same flying height, equal to the nominal value of 11 nm, throughout the actuation of the TFC protrusion until contact is initiated. This simplifying assumption allows for the use of a constant rear air bearing stiffness k_r, which can be calculated from the natural frequencies of the air bearing. As discussed in [5] and [6] the air bearing dynamics are affected by the thermal behavior of the TFC, something that is not considered in the present work. Nevertheless, since the model is using experimental TD measurements to correlate with the model predictions, some of these complex effects are indirectly captured by the model. As the main goal of this study is to use a physics-based dynamic contact model to predict FHM and friction under light contacting conditions, the present assumption is justified.

The natural frequencies of the specific air bearing used in the present study were found to be 119.1 and 304.8 kHz for the first and second modes. Modal analysis was then used to calculate the pair of front and rear air bearing stiffness values that yielded the corresponding natural frequencies of the system. These, together with additional model parameters are summarized in Table I.

D. Identification of Contact Criterion

TFC TD experiments were used to investigate the onset of contact and its definition as used in the rough surface contact model. Contact herein is defined as occurring when the separation h (measured from the mean of asperity heights of the two rough surfaces) is smaller than $n \times \sigma$, where n is determined from the TD experiments, and is typically less than 3 (σ is the

TABLE I
DYNAMIC MODEL PARAMETERS

Symbol	Parameter	Value	Unit
a_{TFC}	TFC protrusion half-width	3	μm
b_{TFC}	TFC protrusion height	1-15	nm
w_{TFC}	TFC protrusion width	50	μm
x_{TFC}	TFC protrusion offset from TE	8	μm
nom. FH	nominal flying height	11	nm
m	slider mass	0.8932	mg
J	slider moment of inertia	1.19×10^{-13}	Kg m^2
l	slider length	1.23	mm
l_t	slider thickness	0.30	mm
θ_o	initial pitch-angle	100	μrad
F	suspension preload	14.7	mN
k	suspension stiffness	10	N/m
k_θ	suspension angular stiffness	1.6×10^{-4}	N/m
ζ	suspension damping ratio	0.01	-
ζ_θ	suspension angular damping ratio	0.001	-
ζ_c	contact damping ratio	0.005	-
kf	front air-bearing stiffness	0.1794×10^6	N/m
kr	rear air-bearing stiffness	0.8100×10^6	N/m
ζ_f	front air-bearing damping ratio	0.0075	-
ζ_r	rear air-bearing damping ratio	0.0075	-
t	total lubricant thickness	1.5	nm
T_o	bonded lubricant thickness	0.75	nm
ε	equilibrium spacing	0.098	nm

equivalent root-mean-square roughness). In earlier models, the value of n was selected to be equal to 3 [2], based on theoretical considerations alone. A $3 \times \sigma$ contact criterion represents 0.3% probability of contact (for a normal distribution of asperity heights), which is practically undetectable in a HDI system.

Based on TD experiments with 11 nm nominally flying sliders, the measured TFC protrusion height at which contact was detected was found to be 9.8 nm. To align the measured onset of contact, with the contact criterion in the dynamic contact model, contact was defined as the value of n in the expression $n \times \sigma$ for which, for a TFC protrusion height of 9.8 nm, a "sudden" increase in normal vibration was detected, while, there was no such increase for the previous actuation height of 9.6 nm. A series of dynamic simulations was performed for a fixed b_{TFC} value of 9.8 nm with n values ranging from 0 to 2.8. In the model, contact was identified when the separation becomes less than the contact criterion, i.e., when $h < n \times \sigma$. Based on these results, it was found that the contact criterion is equal to $1.2 \times \sigma$. This means that, for a TFC protrusion height of 9.8 nm and a combined $\sigma = 0.869$ nm, contact first occurs when the separation becomes less than 1.043 nm, while at the previous actuation height of 9.6 nm there is no contact. A way of interpreting this contact criterion is to say that there is a $100\% - 67.2\% = 32.8\%$ probability of contact (or that 32.8% of asperities experience contact, for a normally distributed roughness). This value of the contact criterion was adopted for the remainder of the simulations where b_{TFC} was varied from 0 to 15 nm.

E. TFC Nominal Area of Contact

Using the established contact criterion, the nominal area of contact was calculated based on the exact TFC geometry and pitch of the air-bearing. The instantaneous lowest point of the TFC ellipsoid can come as close as $(3 - 1.2) \times \sigma = 1.8 \times \sigma = 1.564$ nm to the combined rough surface for contact to be initiated. Therefore, the nominal area at the moment of inception of contact can be calculated by hypothetically sectioning the ellipsoid volume with a horizontal plane located at 1.564 nm upward from the lowest point on the ellipsoid. To this end, the TFC ellipsoid geometry is characterized relative to the middle of the trailing edge (a fixed point) using analytical equations. The cutting plane is also described analytically and the system of equations is solved to yield the coordinates of the nominal area of the ellipse in the three-dimensional space. Knowing these coordinates allows for the calculation of its area, while the only variable in the system is the TFC protrusion height b_{TFC}. For example, at TFC pole protrusion heights of 5, 10, and 15 nm, the corresponding protrusion curvatures and nominal contact areas are 1506, 827, 567 μm and 124, 68, 47 μm^2, respectively.

III. EXPERIMENTAL MEASUREMENTS

All measurements were performed at mid-diameter of a 3.5-inch disk ($\mathrm{MD} = 34.25$ mm). Both the dynamic microwaviness and TD identification (contact criterion) measurements used a nominal disk speed of 5425 RPM.

A. DMW

DMW is what the flying slider (in this case the TFC protrusion) will experience as a dynamic input from the rotating disk. The content of such signal includes low wavelength disk topography (waviness) and possibly system dynamics and is measured using a noncontact vibration instrument such as a laser Doppler vibrometer (LDV). An LDV (Polytec PI) with a laser spot size of 15 μm diameter was used to measure the disk profile as the disk was rotated at 5,425 RPM while the laser remained stationary above the disk at the MD. The velocity decoder of the LDV was set at 25 $\mathrm{mm\,s^{-1}/V}$ sensitivity and the output signal was high- passed filtered at 10 kHz, corresponding to spatial wavelengths of 1.95 mm. The highest frequency content of the DMW was 500 kHz, corresponding to spatial wavelengths of 39 μm. Precise triggering was accomplished using a separate laser nanosensor and the data were recorded at 4 MS/s over a distance of 78.55 mm. The signal was then averaged 100 times and subsequently integrated to obtain the displacement. The standard deviation of the measured DMW is 0.918 nm. The larger than expected amplitude is because of the 10-kHz cutoff, which allows higher amplitude larger spatial wavelengths that are "perfectly" tracked by the TFC protrusion. One could use a higher high-pass filter of 20 kHz without affecting the results.

B. Roughness Parameters

An AFM was used to measure the roughness of the disk. The scan size was 10 μm^2 with 512×512 points at a scan rate of 1 Hz. The roughness data were digitized and exported for extraction of the statistical parameters (root-mean-square roughness σ, average radius of curvature of asperities R, areal density of asperities η, and distribution of asperity heights). Table II lists

TABLE II
DISK AND TFC MATERIAL PROPERTIES AND ROUGHNESS PARAMETERS

Symbol	Parameter	Value	Unit
E_{DISK}	disk (DLC) Young's modulus	280	GPa
ν_{DISK}	disk (DLC) Poisson ratio	0.24	-
E_{TFC}	TFC Young's modulus	280	GPa
ν_{TFC}	TFC Poisson ratio	0.24	-
H	disk (DLC) hardness	13	GPa
$\Delta\gamma$	surface adhesion energy	0.055	N/m
σ_{DISK}	disk RMS roughness	0.34	nm
R_{DISK}	disk mean radius of asperity curvature	0.43	μm
η_{DISK}	disk areal density of asperities	220	μm^{-2}
σ_{TFC}	TFC RMS roughness	0.80	nm
R_{TFC}	TFC mean radius of asperity curvature	32.74	μm
η_{TFC}	TFC areal density of asperities	1.77	μm^{-2}
σ	combined RMS roughness	0.87	nm
R	combined mean radius of asperity curv.	0.43	μm
η	combined areal density of asperities	212.42	μm^{-2}

the disk and TFC bulge extracted parameters as well as the combined or equivalent parameters.

C. TD Identification

Flyability measurements were performed using the same disk location and speed as the DMW measurements. A special pattern was written on a data track of the disk and the signal amplitude was measured for sequential actuation steps until TD was detected [1]. The actuation resolution was equal to 0.20 nm. TD was identified using the self-diagnosing (burn-in) mode process of the HDD at the actuation step where a sudden increase of normal vibration was detected. The signal amplitudes were then converted to head media spacing (HMS) values using the procedure in [1]. Using the results of the TD experiments, it was possible to calculate the difference in HMS values between zero actuation and TD. This difference, which is set equal to the TFC protrusion height, by definition includes any thermal or other effects from the TFC actuation.

IV. RESULTS AND DISCUSSION

Simulations were performed for a range of TFC protrusion heights between 0 and 15 nm. The dynamic results—clearance time histories, interfacial forces, contact pressure and shear stress—are first presented and then averaged over the steady state range and plotted against the TFC protrusion height. Time histories of the clearance for flying (TFC protrusion height of 9.6 nm) and steady, light contact (TFC protrusion height of 11 nm) operating conditions are presented in Fig. 3. In the rough surface interacting model considered in this work, clearance is defined as the distance between the instantaneous lowest point of the TFC protrusion and the disk surface. From the previous definition of contact, i.e. $h < n \times \sigma$ for contact to occur, the clearance can be obtained as $h - n \times \sigma$ where h is the separation equal to the difference between the instantaneous values of the slider displacement z_t and the DMW z_{dt}, while $n \times \sigma$ is equal to 1.043 nm; hence, contact exists when clearance is negative (onset of contact is at zero clearance). The magnitude of the negative clearance during contact is termed interference. As seen in Fig. 3(a), no contact is encountered; however, there is significant FHM, whereas Fig. 3(b) shows sliding light

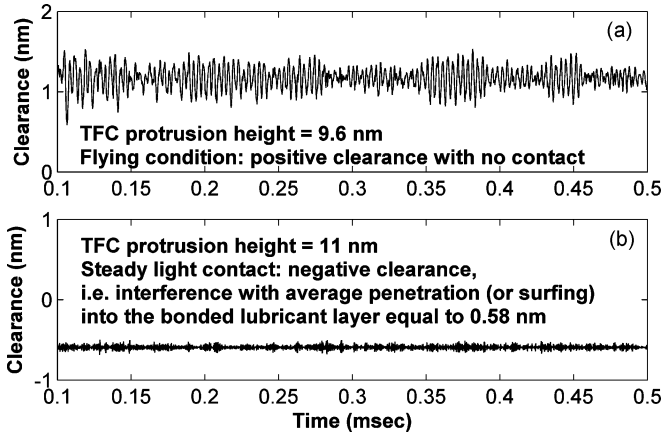

Fig. 3. Time histories of TFC clearance. (a) TFC pole tip height of 9.6 nm. (b) TFC pole tip height of 11 nm.

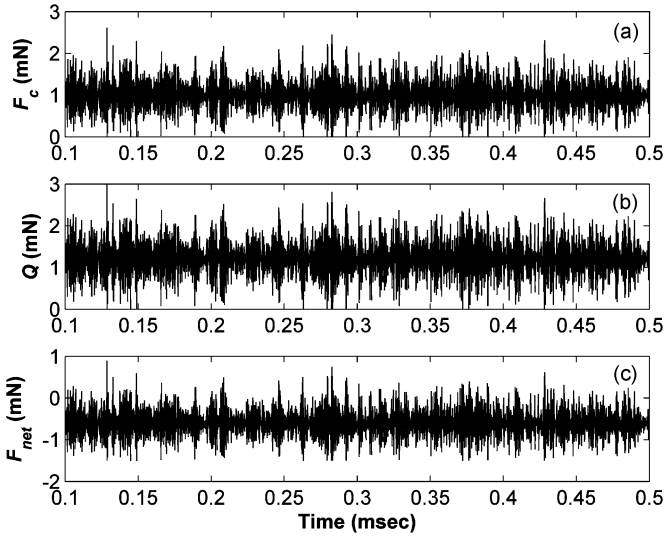

Fig. 4. Dynamic interfacial forces for 11 nm TFC protrusion. (a) Contact force. (b) Friction force. (c) Net normal force.

contact without significant bouncing vibrations. The average interference is 0.6 nm, corresponding to lubricant contact only, i.e., surfing recording.

As the model can predict stable light contact, which has also been observed experimentally using TFC technology [7], next we investigate the interfacial forces corresponding to these conditions. The contact, friction and net interfacial forces—time histories for mild, steady contact operating regime [Fig. 3(b)]—are depicted in Fig. 4, while the corresponding friction coefficient (friction force divided by the contact force), mean contact pressure (contact force divided by the real area of contact) and shear stress (friction force divided by the real area of contact) time histories, all of which are calculated form the dynamic interfacial forces, are shown in Fig. 5. The instantaneous contact force, Fig. 4(a), has an average value of about 1 mN, while the friction force is slightly higher, thus resulting in an average friction coefficient of about 1.2, Fig. 5(a). It should be emphasized that this is a calculated friction coefficient based on the contacting/sliding asperities and the generated stresses and there is no preassumed value.

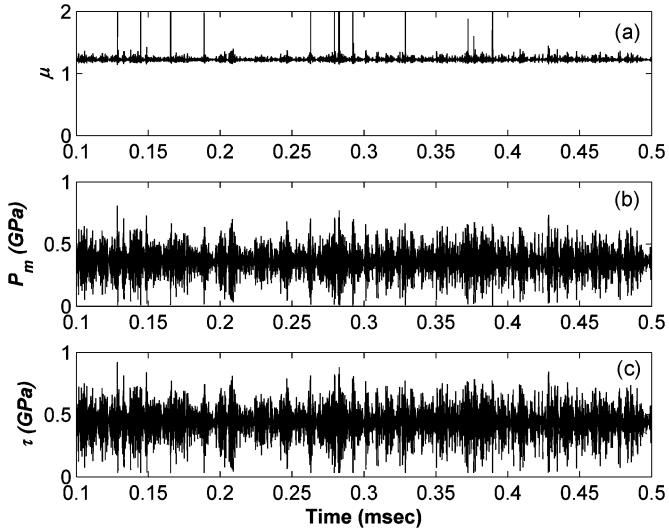

Fig. 5. Dynamic interfacial parameters for 11 nm TFC protrusion. (a) Friction coefficient. (b) Mean pressure. (c) Shear stress.

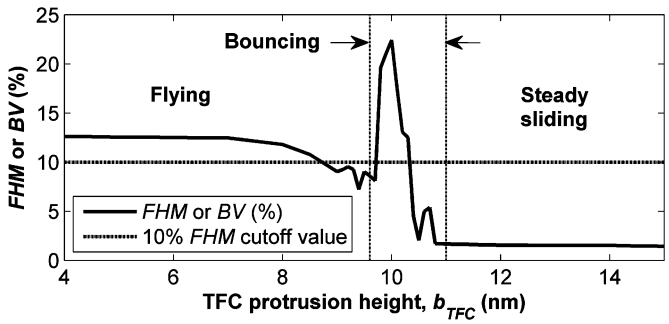

Fig. 6. FHM/BV versus TFC protrusion height showing flying, bouncing, and steady sliding surfing regimes.

The net interfacial normal force, Fig. 4(c) includes the contact, damping and adhesive forces and its average negative value indicate a net attractive force due to adhesion. The mean contact pressure and average shear stress at the sliding interface is of the order of 400 MPa, which is significantly lower than the values predicted for sliders without TFC technology [8], despite the lower values of interacting nominal and real areas of contact. The main reason for the lower values is that the interacting nominal and real areas of contact are lower. Specifically at 11 nm TFC actuation, the nominal contact area is 62 $\mu\mathrm{m}^2$ and the real area of contact is only 2.7 $\mu\mathrm{m}^2$ (4.3%).

A. FHM and Bouncing Vibrations

The instantaneous dynamic separation can be used to calculate the FHM—while the slider is flying—or bouncing vibration (BV)—during contact—at the TFC protrusion from

$$FHM(\%) \text{ or } BV(\%) = \frac{\max(h) - \min(h)}{\text{Nominal } h}. \qquad (1)$$

It is perceived that FHM should be limited to less than 10% for stable flying and reliable recording performance. Fig. 6 depicts the FHM and BV versus TFC protrusion height. This plot was obtained from multiple time-varying displacement histories over the whole range of 15 nm TFC actuation.

At a TFC protrusion height of 4-7 nm (corresponding to clearances of 5.8 to 2.8 nm) the FHM is about 12.5% and subsequently it decreases for lower clearances until initial TD at 9.8 nm of TFC actuation (Fig. 6). Within the next 5 actuation steps (TFC height of 9.8 to 10.8 nm) significant bouncing vibrations occur exceeding 20% until stable mild contact is established for a TFC protrusion height of 11 nm (which corresponds to 0.58 nm of interference, thus operating in the bonded lubricant layer that is 0.75 nm thick). These simulation results correlate extremely well with the experimental measurements reported in [7] who discern three distinct regimes of the slider's flying behavior: "steady flying with adequate clearance, bouncing motion following the onset of head-disk contact, and steady sliding in the interference regime [7]."

Based on these results, two possible *optimum* operating points could be identified: the first would be at 9 nm TFC protrusion height (0.8 nm prior to TD) where the FHM is 9% while the average clearance is 2.4 nm; the second would be at 11 nm TFC protrusion height (1.2 nm after TD) where the BV is less than 2% and the interference is 0.6 nm (Fig. 3(b)). The two operating conditions correspond to the in-flight and in-contact recording regimes discussed by Liu *et al.* [5]. The first optimum operating point corresponding to 0.8 nm of clearance may be sufficient for Tbit/in^2 recording however FHM is significant and may be unacceptable. Such an operating point could be reached by actuating the TFC until the first significant vibrations due to TD are detected and then retracting the TFC by less than 1 nm to obtain stable flying with reduced FHM. In contrast, the viability of operating at 0.6 nm interference and less than 2% BV, which could potentially yield even greater recording densities, depends on the contact severity and thus possible wear. Next, the dynamic interfacial forces and stresses are analyzed to investigate contact severity.

B. Mean Contact Pressure and Shear Stress

As discussed above, at a TFC actuation height of 11 nm there is mild, steady sliding contact. The interference of 0.58 nm is similar to what reported by Yu *et al.* [4] who, using a single degree-of-freedom HDI model with a potential energy-based formulation, reported that surfing recording, i.e., slider-lubricant contact as detailed by Liu *et al.* [5], corresponds to a stable equilibrium interference of 0.78 nm.

To gain insight on wear, the shear stress is calculated from the dynamic interfacial forces as the ratio of Q/A_r. Fig. 7 presents the trend of the shear stress relative to TFC actuation height during contact, which increases with TFC actuation past TD. The same trends are exhibited by the mean contact pressure as well as the dynamic contact and friction forces, while the real area of contact remains roughly equal to 2.72 $\mu\mathrm{m}^2$ once mild contact is established and maintained.

The average mean pressure is $P_m = 359\,\mathrm{MPa}$ (and the Hertz maximum contact pressure is $P_0 = 1.5P_m \approx 540\,\mathrm{MPa}$) while the shear stress $\tau = 438\,\mathrm{MPa}$, which is significantly lower than the bulk DLC shear strength of 7 GPa. Therefore, with these values, which are smaller than those predicted by Suh *et al.*

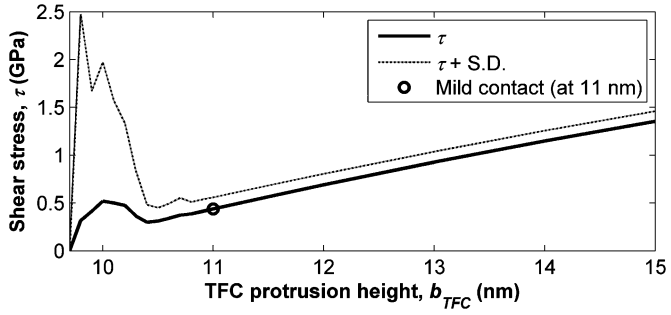

Fig. 7. Shear stress versus TFC protrusion height from the onset of contact to the contacting regime.

TABLE III
SUMMARY OF DYNAMIC RESULTS

b_{TFC} (nm)	Condition	Clearance (nm)	*FHM* or *BV* (%)	P_m (MPa)	τ (MPa)
9.6	Flying	1.04	8.6	-	-
9.8	Touch down	0.70	19.6	257	317
10	Largest *BV*	-0.03	22.4	438	519
10.4	Mildest contact	-0.59	4.54	240	298
11	Steady contact	-0.58	1.68	359	438

[8], it is safe to assume that, while the lubricant is displaced during mild contact, there is not expected significant wear of the DLC layer. This is also confirmed by the plasticity index (defined as the ratio of reduced Young's modulus to Hardness times the square root of σ/R) which is 0.52 (purely elastic contact). The clearance, FHM/BV, P_m and τ values are summarized in Table III for near contact to mild contact or surfing recording conditions.

V. CONCLUSION

Dynamic simulations were performed using a dynamic contact with friction HDI model that accounts for the TFC geometry with input from experimental measurements of DMW and disk roughness parameters. The contact criterion was established in the model based on information from experimental TD measurements. Two possible optimum operating regimes were identified for Tbit/in^2 recording densities based on the simulation results: The first involves the actuation of the TFC until TD is detected and retracting it by less than a nanometer so that the FHM is acceptable and sub-nm clearance is achieved. The second possibility is to actuate the TFC further than TD—but within the lubricant regime—until mild contact or surfing is obtained with BV less than 2%. The contact regime is such that disk wear is expected to be minimal and surfing recording is achieved.

ACKNOWLEDGMENT

The authors would like to acknowledge the support of INSIC Extremely High Density Recording program and J.-K. Lee and S. M. Yeo, Microtribodynamics Laboratory, University of Illinois at Urbana-Champaign, for their help with the DMW and topographical roughness measurements.

REFERENCES

[1] S.-C. Lee and B. D. Strom, "Characterization of thermally actuated pole tip protrusion for head-media spacing adjustment in hard disk drives," *J. Tribol.*, vol. 130, p. 022001-1, 2008.

[2] S.-C. Lee and A. A. Polycarpou, "Microtribodynamics of pseudo-contacting head-disk interfaces intended for 1 Tbit/in^2," *IEEE Trans. Magn.*, vol. 41, pp. 812–818, 2005.

[3] D. Chen and D. B. Bogy, "Dynamics of partial contact head disk interface," *IEEE Trans. Magn.*, vol. 43, pp. 2220–2222, 2007.

[4] S. K. Yu, B. Liu, W. D. Zhou, W. Hua, and L. Gonzaga, "Head disk interface dynamic stability analysis for surfing recording," in *Proc. APRMC 2009 Dig.*, 2009.

[5] B. Liu, M. S. Zhang, S. K. Yu, W. Hua, C. H. Wong, W. D. Zhou, Y. J. Man, L. Gonzaga, and Y. S. Ma, "Towards fly- and lubricant-contact recording," *J. Magn. Magn. Mater.*, vol. 320, pp. 3183–3188, 2008.

[6] B. Knigge, O. Ruiz, and P. Baumgart, "Minimum stable flying height with thermal protrusion actuation," presented at the Asia-Pacific Magn. Rec. Conf. (APMRC), Piscataway, NJ, Nov. 29–Dec. 1, 2006, 08855-1331.

[7] Z. Fan, Z. Zhang, and H. Tang, "Study of head-disk interaction and spacing based on readback signal," in *APMRC 2009 Dig.*, 2009.

[8] A. Y. Suh, C. M. Mate, R. N. Payne, and A. A. Polycarpou, "Experimental and theoretical evaluation of friction at contacting magnetic storage slider-disk interfaces," *Tribol. Lett.*, vol. 23, pp. 177–190, 2006.